Versatility of the dipolar filter selection: From 1H nuclear spin diffusion experiment to the measurement of nuclear Overhauser effect in homopolymer melts

Marianne Gaborieau, Robert Graf, Hans Wolfgang Spiess

Versatility of the dipolar filter selection: from ^{1}H nuclear spin diffusion experiment to the measurement of nuclear Overhauser effect in homopolymer melts

Marianne GABORIEAU[1, 2], Robert GRAF[1], Hans Wolfgang SPIESS[1]*

1 Max Planck Institute for Polymer Research, Ackermannweg 10, 55128 Mainz, Germany

2 current address: Key Centre for Polymer Colloids, School of Chemistry, The University of Sydney, NSW 2006, Australia

** corresponding author, spiess@mpip-mainz.mpg.de*

dedicated to Prof. Jerzy Blicharski

Address for the manuscript correspondence:
Prof. Hans Wolfgang SPIESS
Max Planck Institute for Polymer Research
Ackermannweg 10
55128 Mainz
Germany
tel: +49 61 31 379 120
fax: +49 61 31 379 320
e-mail: spiess@mpip-mainz.mpg.de

Abstract

Dipolar filters select ^{1}H magnetization according to local dipolar dephasing, which corresponds to site mobility in systems with heterogeneous molecular mobility. Combined with a conventional exchange experiment, it is usually applied to polymeric samples exhibiting structures on the nanometer length scale associated with a strong dynamic contrast. There, the resulting ^{1}H nuclear spin diffusion experiment yields the size of the structure. When the same experiment is applied to homopolymer melts exhibiting a weak dynamic contrast and dynamic heterogeneities on significant shorter length scales, the recorded magnetization decay is in agreement with decays expected from a heterogeneous nanostructure. However, dipolar filters actually can also select mobile parts of the repeat unit, e.g. the end of the alkyl side chains and the subsequent magnetization transfer then can occur via cross relaxation due to non coherent zero-quantum transitions (nuclear Overhauser effect, NOE). The difficulties of distinguishing these two cases are examined and it is demonstrated that NOE experiments exploiting magnetization selection via the dipolar filter allow quantifying the local dynamics of the side chains. This opens new possibilities for measurements of local dynamics in non isotopically labeled homopolymer melts.

Keywords

solid state NMR, dipolar filter, spin diffusion, nuclear Overhauser effect, NOE, local dynamics, homopolymer melt, poly(ethyl methacrylate), polymethacrylate.

Introduction

Heterogeneous molecular mobility in polymeric systems plays an important role in various macroscopic application properties. Several solid-state NMR methods can be used to characterize these systems.[1] For instance, the dipolar filter [2] selects ^{1}H magnetization according to local dipolar dephasing, which corresponds to the site mobility. Combination with a conventional exchange experiment results in a so-called "spin diffusion" experiment. [3] The term "spin diffusion" describes the transport of spin polarization between spatially separated equivalent spins [4] and it usually occurs without material transport. The original idea of a spin diffusion experiment was introduced by Goldman and Shen.[5] Apart from local mobility, the selection in spin diffusion experiments can be done according to various other criteria, including $T_{1\rho}$ relaxation time or ^{1}H chemical shift. [6][7][8] The ^{1}H nuclear spin diffusion with dipolar filter has been applied already to numerous polymer samples, including block copolymers,[3] blends,[3] core-shell particles[9][10] and conetworks (polymer chains covalently bonded by blocks of another polymer) [11]. The different samples had in common a phase separation on the nanometer length scale in the material, leading to the formation of two phases composed of one homopolymer each. ^{1}H nuclear spin diffusion with dipolar filter allowed to quantify the size of these structures.

Heterogeneous molecular mobility was recently revealed in poly(n-alkyl methacrylate) melts. X-ray scattering studies [12][13][14] as well as solid-state NMR studies [15] of the melt state of poly(n-alkyl methacrylates), and in particular poly(ethyl methacrylate), indicated a tendency of local nanophase separation between the polar, less flexible backbones and the non polar, more flexible side chains. The experimental results are consistent with an alternation of main chain layers and side chain layers a few monomeric units long as limiting structure, resulting in organized domains of the size of a few nanometers. This structure could be associated with a dynamic contrast between more mobile side chains rich areas and the less mobile main chain dominated parts of the sample.

Therefore, in the present work, poly(ethyl methacrylate) melts were investigated by a combination of dipolar filter with conventional exchange experiment. Poly(ethyl methacrylate) melts represent a new kind of sample for this technique. Previously investigated polymeric samples exhibited typically two glass transition temperatures, each corresponding to one phase, and the difference between the T_g values ranged from 80 K to 175 K. In all cases, the experimental results have been obtained at an intermediate temperature between the two T_gs. This implied a high difference of mobility between the two phases at the

measurement temperature, i.e. a high mobility contrast and thus a significant difference in residual dipolar couplings. In those cases, the more mobile phase exhibited a line narrower than the one of the less mobile one by at least an order of magnitude. In the present work, the same technique was applied to homopolymers in the melt. All samples exhibited a single T_g and a low mobility contrast, as concluded from ^{1}H and 2D-WISE spectra. In homopolymer melts close to T_g, dynamic heterogeneities have been detected and their sizes have been determined by combining conventional spin diffusion with reduced 4D exchange experiments.[16] The question then arises, whether similar experiments can be performed at somewhat higher temperatures, applying the dipolar filter as a source of selection. Moreover, care has to be taken to distinguish magnetization exchange from cross-relaxation via the nuclear Overhauser effect (NOE),[17] which occurs on a molecular level. Such experiments are described below emphasizing the difficulties of distinguishing these two cases from incomplete data sets and describing ways to avoid them.

Materials and Methods

Samples description

The synthesis of the poly(ethyl methacrylate) samples by conventional free-radical polymerization in solution was described elsewhere.[18] The samples investigated in the present work were, respectively, non isotopically labeled (PEMA), fully deuterated on the main chain (PEMADMC), and 20 % ^{13}C statically labeled on the carbonyl group (PEMA13C). Chemical structures are shown on Figure 1 and the results from characterization given in Table 1. The glass transition temperatures, T_g, were determined using differential scanning calorimetry (DSC) at 10 $K \cdot min^{-1}$ and molar masses via size exclusion chromatography (SEC) in THF, calibrated with PMMA standards and the Mark-Houwink-Sakurada parameters ($K=9.44 \cdot 10^{-5}$ $dL \cdot g^{-1}$and $\alpha=0.719$ for PMMA, $K=9.70 \cdot 10^{-5}$ $dL \cdot g^{-1}$and $\alpha=0.714$ for PEMA) [19].

NMR experiments

Solid-state NMR measurements were carried out on a Bruker DSX spectrometer at Larmor frequencies of 300.13 MHz for ^{1}H and 75.47 MHz for ^{13}C using commercial 7.5 mm static and 4 mm magic angle spinning (MAS) double resonance probes from Bruker BioSpin GmbH. All spectra were externally referenced through adamantane (^{1}H chemical shift at 4.64 ppm, ^{13}C CH chemical shift at 38.5 ppm). For the measurements done under static conditions,

the actual sample temperature was calibrated using lead nitrate [20] and a few melting points (due to the lack of proper standard to calibrate the ^{207}Pb ppm scale [21]).[22]

^{1}H spectra were recorded using single pulse excitation under static conditions in a 7 mm rotor, with 62.5 kHz RF nutation frequency corresponding to a 4 µs 90° pulse length, 16 transients and 5 s recycle delay. Temperatures ranged between T_g-45 K and T_g+115 K for PEMA, T_g-45 K and T_g+129 K for PEMADMC, T_g-46 K and T_g+128 K for PEMA13C.

A 2D-WISE spectrum [23] was recorded under static conditions on PEMA13C at T_g+81 K using a 7 mm rotor. A 5 µs 90° ^{1}H pulse was used, followed by a 180° pulse in the middle of indirect time to refocus the chemical shifts, in order to acquire the static ^{1}H line width in the indirect dimension. In order to avoid ^{1}H spin diffusion, polarization transfer from ^{1}H to ^{13}C was accomplished by Lee-Goldburg cross-polarization, with 500 µs contact time. During ^{13}C acquisition, ^{1}H continuous wave decoupling at 50 kHz RF nutation frequency has been applied. 160 increments were acquired in the indirect ^{1}H dimension and 256 transients were recorded in the direct ^{13}C dimension with 2 s relaxation delay between consecutive transients.

Experiments monitoring the decay of magnetization in the more mobile parts of the sample after a dipolar filter [2] were carried out under static conditions (s. Figure 2 for pulse scheme). 62.5 kHz RF nutation frequency and 5 s recycle delay were used. The delay τ between pulses in the dipolar filter was varied from 10 to 20 µs, and the number n of cycles in the dipolar filter from 1 to 12, depending on the sample and the temperature. The measurements were carried out at temperatures ranging from T_g+55 K to T_g+115 K on sample PEMA, from T_g+60 K to T_g+100 K on sample PEMADMC.

Lee-Goldburg CP MAS spectra were recorded at 3 kHz MAS spinning frequency using 4 mm rotors. In the ^{1}H channel the RF power level was set to a nutation frequency of 83 kHz (corresponding to a 90° pulse length of 3µs) for excitation as well as for ^{1}H continuous wave decoupling during acquisition. A relaxation delay of 3 s was chosen for these experiments. The Lee-Goldburg irradiation [24] for the CP was adjusted on the ^{1}H nuclei by first calculating the corresponding irradiation offset frequency for the chosen RF power level and then finely adjusting the irradiation power by optimizing the resolution of ^{13}C multiplets under Lee-Goldburg decoupling conditions. The following series of experiments was conducted (s. Figure 3): first a simple LG-CP spectrum, second a LG-CP spectrum recorded immediately after a dipolar filter, third a LG-CP spectrum recorded after a dipolar filter with the same experimental settings and a subsequent mixing time. The experiments were conducted on PEMA at ca 390 K (ca T_g+45 K) with a CP contact time of 500 µs, a filter with 20 µs delay and 1 cycle, mixing times of 1 ms and 50 ms, and 1 536, 25 600, 32 768, 46 080

transients for the four spectra, respectively. The experiments were conducted on PEMADMC at ca 390 K (ca T_g+45 K) with a CP contact time of 500 µs, a filter with 10 µs delay and 1 cycle, a mixing time of 8 ms, and respectively 4 096, 8 192, 15 360 transients for the three spectra.

Results and Discussion

Dynamic contrast in PEMA

The dynamic contrast, the difference in mobility between the more mobile and the less mobile parts of a sample, can be characterized by ^{1}H static spectra and two dimensional wide-line separation (2D-WISE) experiments. A few representative ^{1}H spectra are shown for sample PEMA in Figure 4. At none of these temperatures, a simple superposition of a broad and a narrow line is observed. Instead, the line becomes narrower in a visually homogeneous way with increasing temperature. This means that the whole sample becomes more mobile with increasing temperature, and exhibits no significant dynamic contrast. However, weak dynamic contrast within the sample might still be present and probed using the dipolar filter. In that case, the static spectra would be a superposition of lines with similar line widths, so that it would be difficult to visually differentiate them. The same experimental results were obtained for samples PEMA13C and PEMADMC (data not shown [22]).

The 2D-WISE technique [23] was used in order to characterize more precisely the dynamic contrast in molten poly(ethyl methacrylate) with a higher structural resolution. In a 2D-WISE spectrum the different sites of the molecule are resolved according to their chemical shifts in the ^{13}C (direct) dimension and are correlated with the line width in the ^{1}H (indirect) dimension. This experimental procedure provides information on the mobility of the corresponding site: the narrower the line, the more mobile the chemical site. 1D ^{1}H spectra extracted from the 2D-WISE spectrum of sample PEMA13C at T_g+81 K are presented on Figure 5. The lines exhibited the following order for decreasing mobility: side chain CH_3, then main chain CH_3, then CH_2 groups. It should be pointed out that apparent differences in mobility are obscured by possible ^{1}H nuclear spin diffusion during the CP contact time.[23] Therefore Lee-Goldburg CP, providing ^{1}H homonuclear decoupling during the CP contact time and thus suppressing spin diffusion, was used here.[24][25] However, an accurate adjustment of the Lee-Goldburg conditions is only possible under MAS, due to the presence of heteronuclear dipolar couplings under static conditions. The ^{1}H nuclear spin diffusion would thus not be completely suppressed but only weakened in the 2D-WISE recorded here

under static conditions. It should be noted that main chain and side chain CH_2 groups cannot be differentiated in this experiment because of the poor spectral resolution in the ^{13}C dimension.

Combination of the dipolar filter with a conventional exchange experiment applied to investigate poly(ethyl methacrylate)

Poly(ethyl methacrylate) melts were investigated by a combination of the dipolar filter [2] and a conventional exchange experiment (s. Figure 2 for pulse scheme), monitoring the decay of ^1H magnetization of the more mobile parts after the dipolar filter. This investigation of samples with low mobility contrast required several changes in the data processing and analysis, which are presented below, after a short description of the usual procedure for a spin diffusion experiment.

In the conventional ^1H nuclear spin diffusion experiment, several FIDs are recorded as a function of mixing time τ_m and Fourier transformed. For increasing τ_m, a broad line of increasing area appears below the narrow line present at the end of the dipolar filter, indicating that magnetization has diffused to a less mobile component. Furthermore, the total intensity (line area) decreases, due to longitudinal relaxation T_1. In the usual case of a high mobility contrast, the decay of the intensity of the more mobile ^1H magnetization is monitored as the area of the narrow line by integration of the signal in the corresponding spectral window.[3] The monitored decay is due to two factors: magnetization transfer to less mobile parts and T_1 relaxation. In order to distinguish magnetization transfer and T_1 relaxation, the magnetization is alternatively stored along +z and –z during the mixing time τ_m, and the corresponding transients are subtracted.[7] To correct the data for T_1 relaxation, the recorded intensity of the more mobile parts is divided by the intensity obtained for the same mixing time without application of the dipolar filter.[8][3] The so-corrected intensity is then normalized by the initial intensity (extrapolated at τ_m=0 from the linear initial slope as a function of the square root of the mixing time). The final curves are plotted as a function of the square root of the mixing time; they exhibit a linear behavior for short mixing times and a plateau for the long ones. According to the Babinet's principle, the initial decay does not exhibit any difference between the case of less mobile domains in a more mobile matrix and the inverse case.[7] The plateau value corresponds to the percentage of selected magnetization after application of the dipolar filter (it usually slightly depends on the filter parameters due to the presence of an interphase with mobility gradient rather than a sharp interface between the

more and the less mobile parts [9]). From the intercept of the initial slope with the X-axis, $\sqrt{\tau_m^*}$, the domain size d_{size} of the underlying structure (lamella thickness, cylinder or sphere diameter) can be calculated, according to equation 1, where ε is the dimensionality (1 for lamellae, 2 for cylinders and 3 for spheres), and D_{eff} the effective ^{1}H nuclear spin diffusion coefficient through coherent magnetization transfer.

$$d_{size} = \frac{2 \cdot \varepsilon}{\sqrt{\pi}} \cdot \sqrt{D_{eff}} \cdot \sqrt{\tau_m^*} \tag{1}$$

D_{eff} is calculated from the ^{1}H nuclear spin diffusion coefficients of the more mobile and less mobile phases D_{mob} and D_{rig} according to equation 2.

$$\frac{1}{\sqrt{D_{eff}}} = \frac{1}{2}\left(\frac{1}{\sqrt{D_{mob}}} + \frac{1}{\sqrt{D_{rig}}} \right) \tag{2}$$

D_{rig} is usually taken equal to the value measured for polystyrene below its T_g (0.8 $nm^2 \cdot ms^{-1}$), while D_{mob} can be determined using its correlation with the transversal relaxation time T_2.[3] The T_2 relaxation time of the more mobile phase has to be measured independently, either using the Carr-Purcell-Meiboom-Gill (CPMG) experiment [26][27], or by measuring the line width of the static ^{1}H spectrum assuming a Lorentzian line shape, in either case just after applying the dipolar filter.

Determining the decay of the intensity of the more mobile ^{1}H magnetization by integration of the signal in a narrow spectral window is not applicable to poly(ethyl methacrylate) melts, because the contrast in mobility (and thus the line width difference) is too low. Therefore, the maximum height of the total ^{1}H spectrum was monitored as a function of the mixing time, which is more sensitive to the narrower component. This estimate allowed us to monitor the time dependence of the magnetization transfer. The absolute values of the degree of exchange, e.g. the plateau value, should, however, be interpreted with care. Concerning the correction for T_1 relaxation, it should be pointed out that the way explained above is valid only if the T_1 value is homogeneous within the sample, or for mixing times much shorter than the shorter T_1 values.[7][28] T_1 relaxation was measured in the samples using the inversion recovery technique [29][30] (data not shown [22]). It exhibited a mono-exponential decay, characteristic of a spatially homogeneous T_1 relaxation, or of samples with a relaxation sink and extensive ^{1}H nuclear spin diffusion. Furthermore, all T_1 times were longer than 800 ms. For all samples, the diffusion curves were processed (initial linear slope

and beginning of the plateau) for τ_m values smaller than 100 ms, thus much smaller that the determined T_1 relaxation values. Therefore the corresponding parts of the ^{1}H nuclear spin diffusion curves could be corrected for T_1 relaxation via division by the corresponding signal without dipolar filter, as detailed above. In poly(ethyl methacrylate) melts, the whole sample was much more mobile than polystyrene below its T_g, so that the less mobile phase could not be assumed to have a spin diffusion coefficient of 0.8 $nm^2 \cdot s^{-1}$. Experimentally, only a single value of spin diffusion coefficient could be determined. Since both phases have similar mobility and ^{1}H spin density, they have similar spin diffusion coefficients. Therefore the average of the spin diffusion coefficient is close to the diffusion coefficient of the more mobile phase. Furthermore, due to the way of averaging, the diffusion coefficient of the more mobile phase has a stronger weight on the average than the other one, since it is lower. Finally, only the diffusion coefficient of the more mobile phase was determined, and assumed to be close to the one of the less mobile phase, thus similar to the average diffusion coefficient. The diffusion coefficient of the more mobile phase was determined via the T_2 relaxation time. Both methods (CPMG experiment, line width) were used for all samples. Only the value calculated from the line width measurement was considered for two reasons. First, the line is broader at the temperature of the ^{1}H nuclear spin diffusion measurements than at higher temperatures (indicating an intermediate mobility). Second, the diffusion coefficients determined through CPMG were higher than the ones determined from the line width of the ^{1}H static spectrum (after a dipolar filter), and both methods overestimate the diffusion coefficient; therefore the lower value was assumed to be more accurate. There was no information on the geometry of the investigated system, since X-ray diffraction detects a smaller structure and the contrast is too low in homopolymers for electron microscopy. In order to minimize the uncertainty, the dimensionality ε was assumed to be 2.

In sample PEMA at T_g+67 K, ^{1}H polarization transfer occurred after the dipolar filter, as indicated by the gradual broadening of the basis of the line with increasing mixing time. The evolution of the ^{1}H magnetization of mobile species with the mixing time after the dipolar filter is shown on Figure 6a. This plot exhibits the typical evolution of the normalized and corrected intensity as a function of $\sqrt{\tau_m}$ in a ^{1}H nuclear spin diffusion experiment using the dipolar filter: a signal decay linear in the square root of the mixing time for small mixing times and a plateau for long mixing times. Processing the data as detailed above for the specific case of polymer melts yielded apparent domain sizes of 3 to 6 nm. Furthermore, the plateau values ranged from 53 to 70 %. Assuming that the dynamic heterogeneity detected by

the dipolar filter is related to nanostructuring in PEMA at T_g+67 K, the quantified size would be in accordance with the typical length of 5 to 10 monomeric units determined in NMR [15] and X-ray scattering [14] studies. However, the actual selection of polarization due to the dipolar filter needed to be checked.

Actual selection done by the dipolar filter and actual subsequent magnetization transfer mechanism

In order to check the actual selection resulting from the application of the dipolar filter, the selected ^{1}H magnetization was transferred to ^{13}C nuclei and acquired in the ^{13}C channel, to gain chemical shift resolution. Obscuring spin diffusion during the magnetization transfer from ^{1}H to ^{13}C nuclei was reduced using Lee-Goldburg cross-polarization (LG-CP, s. above). It would have been best to carry out these experiments under the same conditions as the experiments using the dipolar filter described in the preceding paragraph, namely under static conditions and at T_g+67 K. However, due to the poor chemical shift resolution and the difficulties adjusting Lee-Goldburg irradiation on ^{1}H spins under static conditions, the investigations were conducted under MAS. Due to a limited temperature range of the available MAS probehead, the investigations were conducted at ca 390 K, i.e. ca T_g+45 K. The pulse schemes used to investigate the selection done by the dipolar filter using Lee-Goldburg CP are presented in Figure 3 (left). In the first experiment (a), a simple LG-CP spectrum is recorded to obtain a reference spectrum. In the second experiment (b), a dipolar filter is applied directly followed by LG-CP, in order to determine the parts of the sample actually selected by the dipolar filter. The third experiment (c) corresponds to (b), where a mixing time τ_m is introduced between the dipolar filter and the acquisition of the LG-CP spectrum, in order to observe the relaxation of the sample back to equilibrium. The corresponding spectra for sample PEMA at ca T_g+45 K are shown on Figure 3 (right). The carbonyl signal was too weak to be detected. The ^{13}C LG-CP spectrum (a') exhibited a chemical shift resolution high enough to resolve all the chemical sites of the monomeric unit of PEMA. Furthermore, it gave their reference intensities in a LG-CP spectrum. It is obvious from the ^{13}C LG-CP spectrum (b') that the dipolar filter actually selected essentially the CH_3 group of the side chain of PEMA. Small amounts of other groups were also selected. (It should be noted that this selection of 3 out of 10 ^{1}H nuclei of the monomeric unit of PEMA roughly corresponds to the plateau values of 0.5 to 0.7 observed on Figure 6). The ^{13}C LG-CP spectrum (c') was identical to the one shown in (a'), proving that the magnetization was back at equilibrium 50 ms after the application of the dipolar filter.

In the preceding paragraph, it was assumed for the data processing that the dipolar filter would select mobility contrast due to nanodomains present in PEMA. This would have led to the selection of some whole monomeric units. Therefore it would have resulted in the presence of all the chemical parts of the monomeric units in the ^{13}C LG-CP spectrum recorded after the dipolar filter and no mixing time. However, the LG-CP investigations conducted on PEMA at T_g+45 K clearly showed that the dipolar filter actually selected essentially the CH_3 group of the side chain. This proved that the mobility contrast in PEMA at ca T_g+45 K observed using the dipolar filter did not result from structured and unstructured domains on the nanometer length scale. Instead, the dipolar filter selected the end group of the alkyl side chain only. Similar experiments conducted at ca 390 K (ca T_g+45 K) on sample PEMADMC proved also the selection of the CH_3 group of the side chain only (data not shown [22]).

It was assumed above that the magnetization transfer would have occurred via coherent, energy conserving flip-flops, as it is the case in a typical ^1H nuclear spin diffusion experiment. The LG-CP experiments showed, however, that the dipolar filter selected essentially the end group of the alkyl side chain and that the equilibrating polarization transfer took place from the end group of the alkyl side chain along the alkyl side chain and further to the main chain. Such a magnetization transfer along an alkyl side chain can occur via either coherent or incoherent transfer. In the case of coherent transfer, the residual dipolar couplings would cause zero-quantum transitions, which in the limit of many flip-flop transitions would result in incoherent ^1H nuclear spin diffusion. Incoherent transfer, occurring via incoherent zero-quantum or double-quantum transitions as cross-relaxation caused by fluctuations of the dipolar coupling due to the chain motion, is often termed Nuclear Overhauser Effect (NOE). Since the physical mechanisms behind coherent or incoherent magnetization transfer are completely different, resulting in different time behaviors,[3][31] a quantitative analysis of the experimental data required a detailed knowledge about the dynamic processes in the samples. Fritzhanns et al.[32] investigated the magnetization transfer mechanism in multidimensional NOE experiments carried out on elastomer samples under MAS; they indicated coherent transfer in the case of static measurements, and incoherent transfer in the case of MAS measurements. Demco et al. [33] conducted a detailed study of SBR elastomers at T_g+70 K using NOE experiments under static conditions, and concluded a coherent transfer mechanism in the limit of short mixing times. This leads to a quadratic decay of the magnetization M_z with the mixing time τ_m, described by equation 3, where M_0 was the initial magnetization and <DC> the average residual dipolar coupling.

$$M_z = M_0 \cdot \left(1 - 0.5 \cdot \langle DC \rangle \cdot \tau_m^2\right) \quad (3)$$

The quadratic behavior was experimentally observed for mixing times up to 400 μs. In the present investigation of PEMA at T_g+67 K under static conditions, a coherent transfer of magnetization can be expected for even shorter mixing times, due to the lower molecular mobility of PEMA. However, the time of 400 μs would have been between our second and third experimental point. Furthermore, the magnetization decay of interest in the present study was on the order of several ms (s. Figure 6a), thus of a factor 10 to 100 longer than the time range of coherent transfer. Indeed, plotting our experimental magnetization decays as a function of the square of the mixing time did not result in a linear behavior for very short mixing times (s. Figure 6b). Therefore, it was concluded that in PEMA at T_g+67 K the magnetization transfer after the dipolar filter occurred predominantly via incoherent zero- and double-quantum transitions. Thus the magnetization transfer data obtained in the present work should be processed considering incoherent zero-quantum and double-quantum transitions, i.e. a NOE mechanism. This transfer mechanism results in an exponential decay of the magnetization, as detailed in the following paragraph. Indeed, the linear behavior observed for the recorded magnetization decay after subtraction of the plateau value, normalization and plot on a logarithmic scale (s. Figure 6c) is in agreement with an exponential decay. It should be noted that the magnetization decay caused by ideal zero-quantum transitions in a dense spin ensemble turning into spin diffusion, as calculated from theoretical equations [7], exhibits a quasi-linear behavior when plotted on a logarithmic scale as a function of the mixing time (s. Figure 7c). Therefore, the knowledge about the time dependence of the magnetization decay is not sufficient to discriminate the mechanism of the polarization transfer. However, in the case of PEMA at T_g+67 K, an incoherent cross-relaxation mechanism for the polarization transfer along alkyl side-chain appears to be more likely than the multi-step process, but some coherent contributions to the predominant cross-relaxation transfer in PEMA can not be excluded.

Equation governing the monitored magnetization decay via cross-relaxation

The magnetization transfer after application of the dipolar filter in PEMA at T_g+67 K occurred predominantly via incoherent zero-quantum and double-quantum transitions, i.e. a cross-relaxation or NOE mechanism. Different initial conditions and different transfer conditions are possible for NOE experiments, leading to different equations governing the

magnetization transfer.[17] In the present work, the line height was monitored, which is equivalent to the integral over a thin slice of the spectrum, or to integrate predominantly the mobile component of a superposition of a more mobile component and a less mobile component. Furthermore, in the present experiments, magnetization was present initially only at the more mobile sites, and was transferred in the course of our experiment to all sites depolarized by the dipolar filter. Thus it resembles a 2D NOE experiment where two components A and B would be resolved on the chemical shift scale, where the magnetization would have been selected at A sites initially, where the magnetization would then have been transferred between the sites A and B via cross-relaxation, but only the magnetization of component A would have been recorded. Finally, the present way of monitoring the magnetization decay is equivalent to the integration over time of a diagonal line (A) in a 2D NOE experiment. It should be noted that the present initial conditions (where only the monitored line had magnetization) differ from the classical 2D NOE initial conditions, where all diagonal lines have magnetization. However, "having magnetization" only means that for this particular species, there is excess of spin orientation in one direction of the order of parts per millions. Therefore, it doesn't make a difference for the cross-relaxation at the level of the individual spins, if only one species A has initially magnetization or both species A and B. (see [34]). As a result, the mathematical equations for the time evolution of the diagonal lines intensity in a 2D NOE study [31] directly apply to the present one-dimensional monitoring of the more mobile sites magnetization.

The most elaborate analytical expression describing the evolution of the diagonal line intensity a_{AA} with mixing time τ_m is given by Macura and Ernst [31] for the case of a homonuclear system composed of a group of n_A equivalent A nuclei and a group of n_B equivalent B nuclei. In the investigated samples, the initial magnetization is mainly located at the CH_3 end group of the alkyl side chain. Therefore a CH_3-CH_2 moiety was considered as source of cross-relaxation. It should be emphasized that this is strictly valid for sample PEMADMC, but does not correspond to the whole monomeric unit of sample PEMA; however, to our knowledge, no analytical equation is available for moieties larger than two groups of equivalent nuclei. Moreover, since the initial magnetization is mainly located at the CH_3 end group, the CH_3-CH_2 contribution is expected to be predominant in the initial magnetization decay for sample PEMA. The investigated samples are macromolecules in bulk, therefore they are in the slow motion limit; moreover, they are homonuclear systems. Macura and Ernst [31] did not give explicitly the equation corresponding to that case if n_A is different from n_B; however it could easily be derived from equation 4 [31], where M_0 is the

total equilibrium magnetization of the n_A+n_B nuclei, and the cross-relaxation rates R_{ij} are defined below.

$$a_{AA}(\tau_m) = \frac{n_A M_0}{2(n_A+n_B)} \exp(-R_L \tau_m) \cdot \left[\left(1 - \frac{R_{AA}-R_{BB}}{R_C}\right) + \left(1 + \frac{R_{AA}-R_{BB}}{R_C}\right) \exp(-R_C \tau_m) \right] \tag{4}$$

$$\text{with } R_C = \sqrt{(R_{AA}-R_{BB})^2 + 4R_{AB}R_{BA}} \text{ and } R_L = \frac{1}{2}(R_{AA}+R_{BB}) - \frac{1}{2}R_C$$

The cross-relaxation rates R_{ij} can be expressed by the transition probabilities W, resulting from AA, AB and BB interactions, and by the external relaxation rates R_{1A} and R_{1B}, which take into account possible interactions with further spins (s. equation 5 [31]). In this equation, the subscripts 0, 1(A) and 2 relate respectively to zero-quantum transition, single-quantum transition (with flip on A nucleus), double-quantum transition; the superscripts ij relate to both nuclei involved in the corresponding transition.

$$R_{AA} = 2(n_A - 1) \cdot (W_1^{AA} + W_2^{AA}) + n_B (W_0^{AB} + 2W_{1A}^{AB} + W_2^{AB}) + R_{1A}$$
$$R_{AB} = n_A (W_2^{AB} - W_0^{AB}) \tag{5}$$

The transitions probabilities W obey equation 6 [31], with the spectral densities $J_{xy}(\omega)$ and the constants q_{xy} defined in equation 7 [31]. In the latter, τ_C^{xy} is the correlation time of the isotropic motion which modulates the xy interaction, μ_0 is the permeability of space, γ_x is the magnetogyric ratio of spin x, $\hbar$ is the reduced Planck's constant, and r_{xy} is the internuclear xy distance. Please note that the equation given for the spectral density is obtained for a rigid molecule undergoing isotropic random motions.[36] Moreover, it should pointed out that the investigated phenomenon is local due to its dependence on the inverse sixth power of the internuclear distance.

$$W_1^{xy} = \frac{3}{2} q_{xy} J_{xy}(\omega_x) \qquad W_{1k}^{xy} = \frac{3}{2} q_{xy} J_{xy}(\omega_k)$$
$$W_0^{xy} = q_{xy} J_{xy}(\omega_x - \omega_y) \qquad W_2^{xy} = 6 q_{xy} J_{xy}(\omega_x + \omega_y) \tag{6}$$

$$\text{with} \quad J_{xy}(\omega) = \frac{\tau_C^{xy}}{1+\left(\omega\tau_C^{xy}\right)^2} \qquad \text{and} \qquad q_{xy} = \frac{1}{10}\left(\frac{\mu_0}{4\pi}\right)^2 \frac{\gamma_x^2\gamma_y^2\hbar^2}{r_{xy}^6} \tag{7}$$

The investigated samples are macromolecules in bulk, therefore they are in the slow motion limit and $\omega_X\tau_C >> 1$. The investigated system is a homonuclear system, so that $(\omega_X-\omega_Y)\tau_C \approx 0$, therefore $W_1^{XY}=W_2^{XY}=0$, and the zero-quantum transitions dominate cross-relaxation, with a transition probability of $W_0^{AB}=q_{AB}\cdot\tau_C^{AB}$. The elements of the cross-relaxation matrix can thus be reduced to $R_{AA}=n_BW_0^{AB}+R_{1A}$, $R_{BB}=n_AW_0^{AB}+R_{1B}$, $R_{AB}=-n_AW_0^{AB}$ and $R_{BA}=-n_BW_0^{AB}$. Assuming equal external relaxation rates R_1 for A and B nuclei, the quantities R_C and R_L can then be calculated as $R_C=(n_B+n_A)W_0^{AB}$ and $R_L=R_1$, then $(R_{AA}-R_{BB})/R_C=(n_B-n_A)/(n_A+n_B)$.

With this, the intensity of a diagonal signal is described by equation 8.

$$a_{AA}(\tau_m) = \frac{n_AM_0}{2(n_A+n_B)}\exp(-R_1\tau_m)\cdot\left[\left(1+\frac{n_A-n_B}{n_A+n_B}\right)+\left(1-\frac{n_A-n_B}{n_A+n_B}\right)\exp\left(-(n_A+n_B)q_{AB}\tau_C^{AB}\tau_m\right)\right] \tag{8}$$

In the case of a CH_3-CH_2 moiety, $n_A=3$ and $n_B=2$. Taking the experimental correction of the longitudinal relaxation compensating the exponential factor $\exp(-R_1\tau_m)$ into account, equation 8 is simplified further to equation 9.

$$a_{AA}(\tau_m) = \frac{3M_0}{10}\cdot\left[\frac{6}{5}+\frac{4}{5}\exp\left(-5q_{AB}\tau_C^{AB}\tau_m\right)\right] \tag{9}$$

Thus, the processing of the data $a_{AA}(\tau_m)$ recorded after application of the dipolar filter allows to extract information on the molecular dynamics, via the determination of the correlation time of the involved molecular motion τ_C^{AB}, if the parameter q_{AB} is known.

Several approaches can be used to estimate the coupling strength q_{AB}, i.e. from equation 7 assuming the internuclear distance or considering the second moment for different geometries. As detailed in the Appendix, these values differ but are of the same order of magnitude. Considering the overall uncertainty of our approach, q_{AB}= 9 kHz^2 for PEMA and 6.3 kHz^2 for PEMADMC as deduced from the second moment were used to extract correlation times from the relaxation rates.[37]

Distinguishing different mechanisms of magnetization exchange in dense spin systems

The difficulty to distinguish the different mechanisms of magnetization exchange from the mixing time behavior in dense spin systems is demonstrated in Figure 7. Here the evolution of the ^{1}H magnetization is modelled from the equations given in.[7] The plots demonstrate that magnetization exchange by "spin diffusion" also leads to quasi-exponential behavior at long exchange times. Thus, a definite conclusion how the magnetization exchange curves should be interpreted is not possible from such data alone. In polymers above T_g, however, considerable information about the relaxation times is usually available from other sources, such as dielectric relaxation, light scattering or other NMR methods.[1] In the following we will therefore examine plots like Figure 7 for PEMA at different temperatures and relate them to literature data.[15]

Quantification of local dynamics inside side chains of poly(ethyl methacrylate)

The NOE experiment with dipolar filter was carried out at temperatures ranging from T_g+55 K to T_g+115 K for PEMA, and from T_g+60 K to T_g+100 K for PEMADMC. For each temperature, various parameters were used for the dipolar filter.

At temperatures higher than T_g+85 K for sample PEMADMC and higher than T_g+60 K for sample PEMA, a mono-exponential decay was observed for the recorded magnetization. The data were fitted as a single cross-relaxation process, which follows equation 9: an exponential decay followed by a plateau. In order to fit experimental data, programs were written using the Matlab® (The MathWorks) software, which handled simultaneously a series of measurements done at one temperature using different parameters for the dipolar filter. The plateau value was first determined as the average of all experimental values measured for mixing times longer than a chosen threshold, and subtracted from all experimental values in order to obtain an exponential decay to zero. Then the experimental data were normalized so that the exponential decay begins at 1 for τ_m=0, and fitted with a mono-exponential function (s. equation 10) to extract values for the product $q_{AB}\cdot\tau_C^{AB}$.

$$f(\tau_m) = \exp\left(-5 q_{AB} \tau_C^{AB} \tau_m\right) \tag{10}$$

In the case of PEMA at T_g+67 K, the fits yielded as series of $q_{AB}\cdot\tau_C^{AB}$ values characterized by an average of 275.2 Hz, a range of 15.4 Hz and a standard deviation of 5.6 Hz for the mono-

exponential decay. With q_{AB}= 9 kHz^2 determined from second moment at a temperature well below the glass transition temperature (s. above), a value of $3 \cdot 10^{-5}$ s was obtained for the correlation time τ_C^{AB}. The shape of the curves for high temperatures (above T_g+50 K for PEMA and above T_g+85 K for PEMADMC) were identical to those obtained at T_g+67 K for PEMA, only the numerical values varied. The example of sample PEMA at T_g+115K is given on Figure 8: a linear behavior was observed for the logarithm of the recorded intensity as a function of the mixing time over 15 ms. The obtained correlation times τ_C^{AB} of the dynamic process occurring in the alkyl side chains and giving rise to the cross-relaxation are shown Figure 9 for samples PEMA and PEMADMC.

At lower temperatures, a more complex decay was observed for the recorded magnetization, as shown in Figure 10 for PEMA at T_g+55 K. This behavior could be interpreted as the superposition of two distinct NOE processes with different correlation times, resulting in a bi-exponential decay (s. Figure 10c). It could also be interpreted as a coherent spin diffusion process, as shown by the similarity of the curves shapes in Figures 7c and Figure 10c. The existing data did not allow us to decide between these two interpretations, and the magnetization transfer occurring in the sample was probably a superposition of both processes. The data were fitted using the Microcal™ Origin® software and by a bi-exponential decay. The slow decay was fitted first as a linear decay of the logarithm of the magnetization versus mixing time. Then the fast decay was fitted as one component of a bi-exponential decay where the other component was set as the slow decay determined previously. Note that the slower magnetization decay corresponded to the faster molecular motion, and thus is designated as “fast” in the following. The extracted correlation times are plotted on Figure 9. Please note that the slow process was quantified, while the fast one could be estimated only. The slow process, corresponding to the fast decay, exhibited the same Arrhenius behavior as the single NOE process quantified at higher temperatures (s. Figure 9). Therefore, the complex behavior at lower temperatures was interpreted as the superposition of two independent NOE processes with different correlation times.

The obtained correlation time τ_C^{AB} of the local motion occurring in the alkyl side chains and giving rise to the cross-relaxation are shown Figure 9 for samples PEMA and PEMADMC. It was observed that in the temperature range studied the dependence of τ_C^{AB} on inverse temperature was nearly linear. Furthermore, the values determined for sample PEMADMC were in agreement with those determined for sample PEMA, validating the assumption of the predominance in the initial magnetization decay of the cross-relaxation

from the CH_3 to the CH_2 group along the alkyl side chain. A linear regression of the τ_C^{AB} values yielded a prefactor of 3.10^{-13} s and an activation energy of 27.5 kJ·mol^{-1}. The obtained correlation times are in good agreement with values from literature. The slow and the fast component correspond to chain isotropization and axial chain motion, respectively. Details, as well as complementary results obtained on other poly(n-alkyl methacrylates) and poly(n-alkyl acrylates) will be presented in future publications.

Conclusion

The dipolar filter, combined with a conventional exchange experiment, was applied to homopolymer melts of different poly(ethyl methacrylate) samples. Recent x-ray and NMR studies of these melts indicated the presence of nano-structures in the melt state. However, the melts exhibited only low dynamic contrast originating from the difference in mobility between distinct parts of the monomeric units. In the experiments, the dipolar filter selected only the end of the alkyl side chain, which has been checked using Lee-Goldburg CP experiments. The subsequent ^{1}H polarization transfer was proved to occur via non coherent zero-quantum transition. The NOE processing of our experimental results allowed us to quantify correlation times of dynamics processes in the alkyl side chains. At the lower temperatures, two distinct processes were observed. The determined correlation times are in good agreement with values for the complex chain motion of this polymer known from literature. A sample related interpretation of the detected processes will be presented in a future article, together with results obtained for other poly(n-alkyl methacrylates) and poly(n-alkyl acrylates) melts at various temperatures.

The dipolar filter is used routinely in polymeric samples to quantify domain sizes in phase separated samples. The present work points out processing problems that one should be aware of, if systems with poor phase separation or local structure on a sub nanometer scale are studied. On the other hand, the introduced NOE processing procedure opens a new experimental route to estimate correlation times of local dynamic processes in non isotopically labeled systems using solid state NMR.

Appendix

The q_{AB} constant can be determined by two different approaches. First, it can be calculated according to equation 7, where all the terms are known factors, except the

internuclear distance r_{AB}, which has to be estimated by e.g. molecular modeling. Second, it can be calculated as a value proportional to the second moment [38] of the ^1H line recorded well below T_g under static conditions. The calculation of q_{AB} was done as follows. In the homonuclear ^1H-^1H case, the q_{AB} factor was calculated for an internuclear distance of 1 Å=10^{-10} m from the magnetogyric ratio of ^1H spins ($26.75 \cdot 10^{-7}$ rad·s^{-1}·T^{-1}) [39] and the physical constants $\mu_0/4\pi$ and $\hbar$ (10^{-7} N·A^{-1} and $6.626 \cdot 10^{-34}/2\pi$ J·s^{-1}·rad^{-1} respectively) [40]. This yielded a value of $56.9 \cdot 10^9$ rad^2·s^{-2} i.e. q_{AB}=1.44 s^{-2} for ^1H-^1H and r_{AB}= 1 Å. The actual r_{AB} distance between a ^1H nucleus of the CH_3 and a ^1H nucleus of the CH_2 group was calculated as a function of the involved dihedral angle, then the r_{HH}^{-3} values (proportional to the dipolar coupling) were averaged for equi-distributed values of the dihedral angle between 0 and 360°, which yielded an average distance of r_{HH}=2.67 Å.[22] The calculated q_{AB} parameter was then q_{AB}=3.98 kHz^2 for a CH_3-CH_2 moiety.

Independently, the q_{AB} parameter was measured through the second moment of the ^1H line recorded below T_g under static conditions. The equation describing the q_{AB} factor (s. equation 7, in MKSA unit system) is very similar to the one describing the second moment M_2 of the rigid lattice (s. equation 11, [41][35] in CGS unit system, in the case of a powder of crystalline sample exhibiting a cubic lattice, where I is the spin quantum number, and d the lattice constant).

$$M_2 = \frac{51}{10}\gamma^4\hbar^2 I(I+1)\frac{1}{d^6} \tag{11}$$

Starting from expressions of M_2 in the MKSA unit system [42][43][44], assuming that all nuclei are equivalent,[35] taking the powder average over all orientations,[35] and taking into account the value I=1/2 for ^1H nuclei, the equation 12 was obtained for M_2, where r_{ij} is the internuclear distance between the observed spin and any other one.[22]

$$M_2 = \frac{9}{20}\left(\frac{\mu_0}{4\pi}\right)^2 \gamma^4\hbar^2 \sum_j \frac{1}{r_{ij}^6} \tag{12}$$

The residual sum was simplified considering either an isolated spin pair [45][46] or a simple cubic lattice.[35] The resulting expressions are shown on equation 13.[22]

$$M_2(spin\ pair) = \frac{9}{20}\left(\frac{\mu_0}{4\pi}\right)^2 \gamma^4\hbar^2 \frac{1}{r^6} \quad \text{and} \quad M_2(cubic\ lattice) = \frac{153}{40}\left(\frac{\mu_0}{4\pi}\right)^2 \gamma^4\hbar^2 \frac{1}{r^6} \tag{13}$$

By simple comparison of equations 7 and 13, it was deduced that M_2(spin pair)=4.5 q_{AB} and M_2(cubic lattice)=38.25 q_{AB}. The factor of 8.5 found between the results of the two approaches originates mainly in the presence of 6 next neighbors (and some more remote ones) in the case of the cubic lattice versus a single one in the case of the spin pair. The present case was rigorously neither a spin pair nor a cubic lattice. The geometry of the investigated system was not sufficiently known to draw conclusions on the number and positions of the neighbors. However, several neighbors were present, so that the simple cubic lattice approximation was retained as more realistic. Thus the numerical value of q_{AB} was obtained dividing the experimental value of M_2 by a factor of 38.25.

The numerical integration of a ^1H spectrum recorded under static conditions at T_g-45 K (s. Figure 4 for sample PEMA, data not shown for sample PEMADMC [22]) yielded a second moment value of M_2=342 kHz^2 for PEMA and M_2=240 kHz^2 for PEMADMC; thus values of q_{AB}=9 kHz^2 for PEMA and 6.3 kHz^2 for PEMADMC. Compared to the calculated q_{AB} parameter for a CH_3-CH_2 moiety: q_{AB}=4 kHz^2, the values determined via the second moment were significantly different, but of the same order of magnitude. Considering the overall uncertainty of the present technique, the correlation times were calculated using the q_{AB} parameter value obtained from the experimental second moment exclusively.

Acknowledgements

The authors gratefullly acknowledge the Arkema company (Total group), in particular Francois Beaume and Rene-Paul Eustache, for financial support. We thank Uta Pawelzik for samples synthesis (in particular the synthesis of selectively labeled monomers), Michael Wind and Mario Beiner for sample characterizations and for fruitful discussions, Manfred Hehn and Hans-Peter Raich for technical help with the NMR spectrometers, Manfred Wilhelm and Attila Domjan for discussions, Lothar Brombacher for providing the program allowing the simulation of the ideal spin diffusion curve.

References

[1] K. Schmidt-Rohr, H.W. Spiess, Multidimensional solid-state NMR and polymers, Academic Press Ltd, San Diego, 1994.

[2] N. Egger, K. Schmidt-Rohr, B. Bluemich, W.D. Domke, B. Stapp, J. Appl. Polym. Sci. 44 (1992) 289-295.

[3] F. Mellinger, M. Wilhelm, H.W. Spiess, Macromolecules 32 (1999) 4686-4691.

[4] D. Suter, R.R. Ernst, Phys. Rev. B32 (1985) 5608-5627.

[5] M. Goldman, L. Shen, Phys. Rev. 144 (1966) 321-333.

[6] D.L. Vanderhart, Makromol. Chem. Macromol. Symp. 34 (1990) 125-159.

[7] K. Schmidt-Rohr, H.W. Spiess, Multidimensional solid-state NMR and polymers, Academic Press Ltd, San Diego, 1994, chap. 13, 402-439.

[8] J. Clauss, K. Schmidt-Rohr, H.W. Spiess, Acta Polym. 44 (1993) 1-17.

[9] K. Landfester, H.W. Spiess, Acta Polym. 49 (1998) 451-464.

[10] M. Valtier, X. Drujon, M. Wilhelm, H.W. Spiess, Macromol. Chem. Phys. 202 (2001) 1262-1272.

[11] A. Domjan, G. Erdodi, M. Wilhelm, M. Neidhoefer, K. Landfester, B. Ivan, H.W. Spiess, Macromolecules 36 (2003) 9107-9114.

[12] M. Wind, R. Graf, S. Renker, H. W. Spiess, W. Steffen, J. Chem. Phys. 122 (2005) 014906.

[13] M. Beiner, Macromol. Rapid Commun. 22 (2001) 869-895.

[14] S. Hiller, O. Pascui, H. Budde, O. Kabisch, D. Reichert, M. Beiner, New J. Phys. 6 (2004) 10.

[15] M. Wind, R. Graf, S. Renker, H. W. Spiess, Macromol. Chem. Phys. 206 (2005) 142–156.

[16] U. Tracht, M. Wilhelm, A. Heuer, H. Feng, K. Schmidt-Rohr, and H. W. Spiess, Phys. Rev. Lett. 81 (1998) 2727-2730.

[17] R.R. Ernst, Principles of nuclear magnetic resonance in one and two dimensions, Oxford University Press, Oxford, 1991, chap. 9.7, 516-527.

[18] A.S. Kulik, H. W. Beckham, K. Schmidt-Rohr, D. Radloff, U. Pawelzik, C. Boeffel, H.W. Spiess, Macromolecules 27 (1994) 4746-4754.

[19] S. Beuermann, M. Buback, T.P. Davis, R.G. Gilbert, R.A. Hutchinson, A. Kajiwara, B. Klumperman, G.T. Russell, Macromol. Chem. Phys. 201 (2000) 1355-1364.

[20] P.A. Beckmann, C. Dybowski, J. Magn. Reson. 146 (2000) 379-380.

[21] G. Neue, C. Dybowski, M.L. Smith, M.A. Hepp, D.L. Perry, Solid State Nucl. Magn. Reson. 6 (1996) 241-250.

[22] M. Gaborieau, PhD thesis, University Louis Pasteur, Strasbourg, 2005, available at http://www-scd-ulp.u-strasbg.fr/theses/theselec.html

[23] K. Schmidt-Rohr, J. Clauss, H.W. Spiess, Macromolecules 25 (1992) 3273-3277.

[24] M. Lee, W.I. Goldburg, Phys. Rev. 140 (1965), A1261-A1271.

[25] B.J. van Rossum, C.P. de Groot, V. Ladizhansky, S. Vega, H.J.M. de Groot, J. Am. Chem. Soc. 122 (2000) 3465-3472.

[26] H.Y. Carr, E.M. Purcell, Phys. Rev. 94 (1954) 630-638.

[27] S. Meiboom, D. Gill, Rev. Sci. Instrum. 29 (1958) 688-691.

[28] A.M. Kenwright, K.J. Packer, Chem. Phys. Lett. 173 (1990) 471-475.

[29] E.L. Hahn, Phys. Rev. 76 (1949) 145-146.

[30] M.H. Levitt, Spin dynamics, John Wiley and Sons Ltd, Chichester, 2001, chap. 11, 315-336.

[31] S. Macura, R.R. Ernst, Mol. Phys. 100 (2002) 135-147. Reprint from S. Macura, R.R. Ernst, Mol. Phys. 41 (1980) 95-117.

[32] T. Fritzhanns, D.E. Demco, S. Hafner, H.W. Spiess, Mol. Phys. 97 (1999) 931-943.

[33] D.E. Demco, S. Hafner, C. Fulber, R. Graf, H.W. Spiess, J. Chem. Phys. 105 (1996) 11285-11296.

[34] A. Abragam, The Principles of Nuclear Magnetism, Oxford University Press, Oxford, 1961, chap. VIII, 264-353.

[35] A. Abragam, The Principles of Nuclear Magnetism, Oxford University Press, Oxford, 1961, chap. IV, 97-132.

[36] V.A. Likic, Concepts Magn. Res. 8 (1996) 423-436.

[37] J.S. Blicharski, D. Kruk, App. Magn. Reson. 17 (1999) 367-374.

[38] C.P. Slichter, Principles of Magnetic Resonance, Springer Verlag, Berlin, 1990, chap. 3, 64-85.

[39] R.K. Harris, E.D. Becker, S.M.C. De Menezes, R. Goodfellow, P. Granger, Pure Appl. Chem. 73 (2001) 1795-1818.

[40] K.H. Homann, Abbreviated list of quantities, units and symbols in physical chemistry, http://www.iupac.org/reports/1993/homann/index.html, IUPAC, 1993.

[41] J.H. Van Vleck, Phys. Rev. 74 (1948) 1168-1183.

[42] J. Haase, E. Oldfield, J. Magn. Reson. A101 (1993) 30-40.

[43] Y.L. Wang, P.S. Belton, H.R. Tang, Chem. Phys. Lett. 268 (1997) 387-392.

[44] B. Gee, Solid State Nucl. Magn. Reson. 19 (2001) 73-86.

[45] M. Knorgen, H. Menge, G. Hempel, H. Schneider, M.E. Ries, Polymer 43 (2002), 4091-4096.

[46] P.T. Callaghan, E.T. Samulski, Macromolecules 33 (2000) 3795-3802.

Tables and Figures

Table 1:

Characterization of different poly(ethyl methacrylate) samples

	PEMA	PEMADMC	PEMA13C
T_g [K]	342	345	338
M_n [g·mol^{-1}]	115 000	77 700	55 40
M_w [g·mol^{-1}]	156 200	107 600	122 200
M_w / M_n	1.36	1.38	2.21

Table 1: Glass transition temperatures from DSC and molar masses from SEC in THF of the investigated samples.

Figure 1:

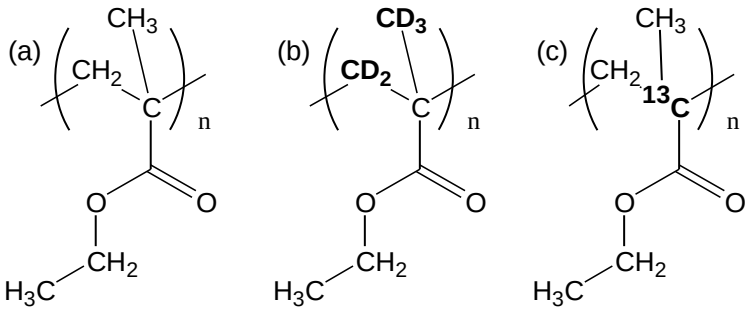

Figure 1: Chemical structure of poly(ethyl methacrylate) samples; (a) PEMA, (b) PEMADMC, (c) PEMA13C. Selective isotopic enrichment is indicated by chemical symbols given in bold fonts.

Figure 2:

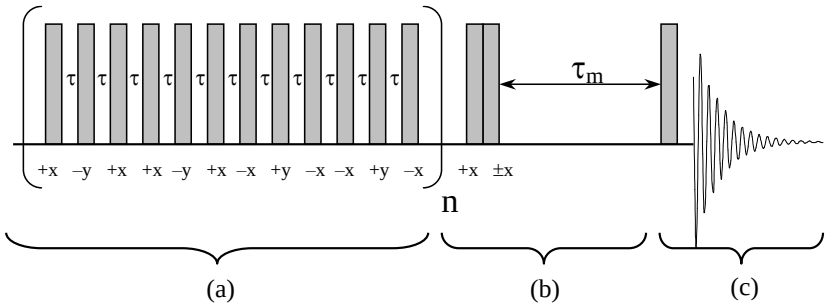

Figure 2: Pulse scheme of the dipolar filter [2] combined with a conventional exchange experiment.[3] At the end of the dipolar filter (a), only the more mobile ^{1}H nuclei of the sample possess magnetization. Then the magnetization remaining in the xy-plane is driven to the z-axis. During the mixing time τ_m (b), transfer of nuclear magnetization occurs. Then the magnetization present along the z-axis is driven to the xy-plane where the FID is recorded (c) and analyzed.

Figure 3:

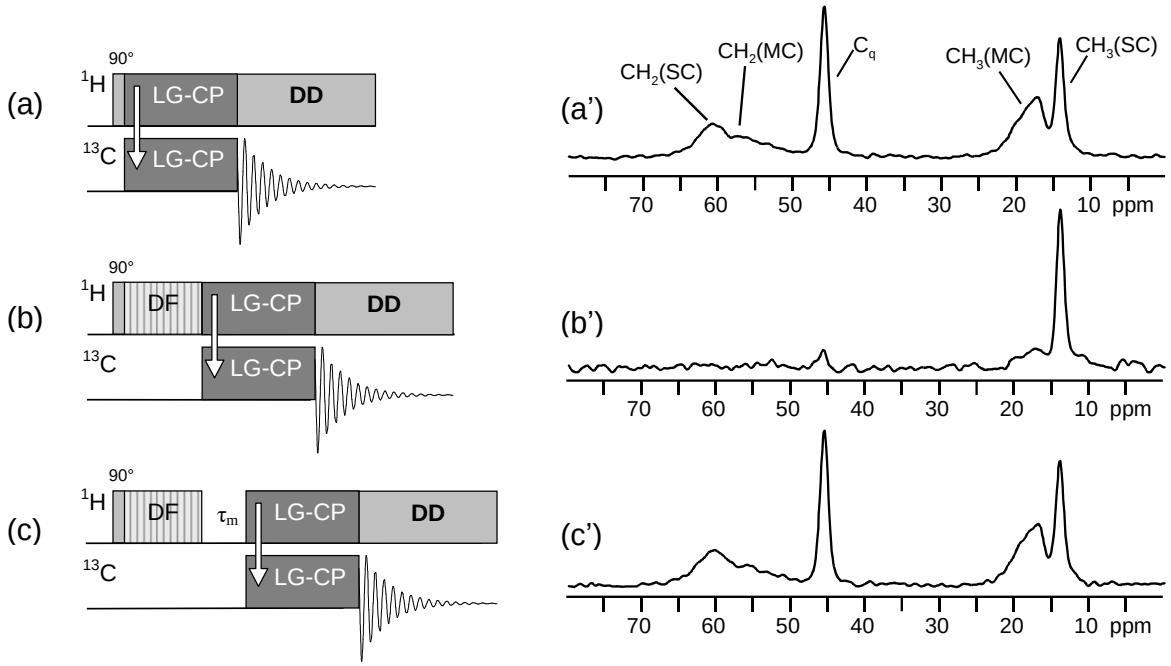

Figure 3: (left) pulse schemes used to investigate the selection done by the dipolar filter in model samples using Lee-Goldburg [24] CP (the abbreviations LG-CP, DD, DF and τ_m designate respectively Lee-Goldburg cross-polarization, dipolar decoupling, dipolar filter and mixing time); (right) corresponding ^{13}C LG-CP spectra of sample PEMA at ca 390 K under 3 kHz MAS (the abbreviations MC, SC and q designate main chain, side chain and quaternary respectively). The mixing time for spectrum (c') is τ_m= 50 ms.

Figure 4:

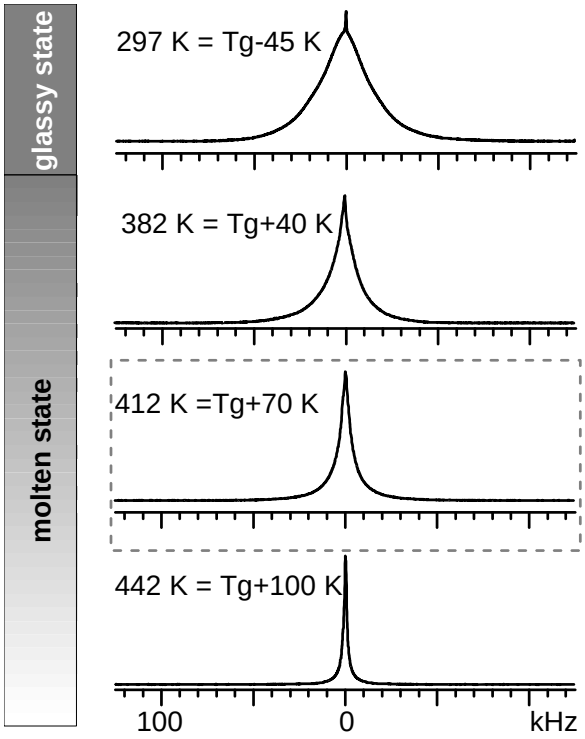

Figure 4: Influence of the temperature on the shape of the ^{1}H spectrum of sample PEMA (recorded under static conditions); the dotted frame indicates the temperature at which the investigation using the dipolar filter was carried out first. Note that the very narrow line below T_g most probably originates from small molecules present in the sample and not from the sample itself.

Figure 5:

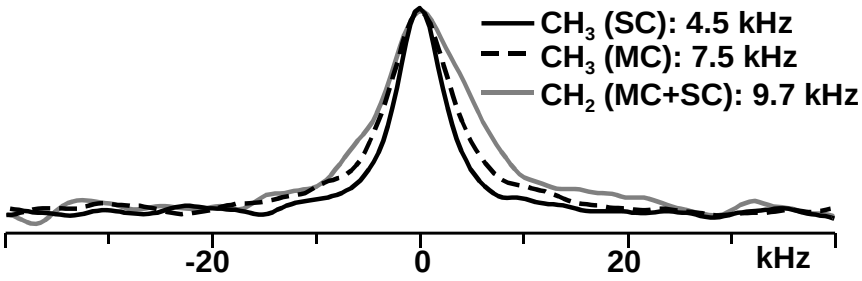

Figure 5: 1D ^{1}H static spectra extracted from 2D-WISE spectra [23] of sample PEMA13C at T_g+81 K under static conditions; the respective full widths at half maximum are indicated (the abbreviations MC and SC designate main chain and side chain respectively, s. Figure 3 for chemical shifts assignments).

Figure 6:

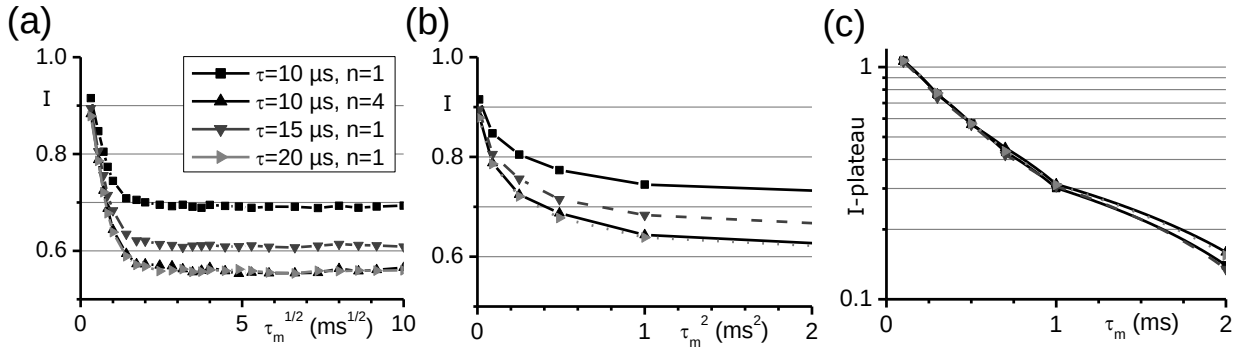

Figure 6: Evolution of the ^{1}H magnetization of mobile species with the mixing time for the sample PEMA at 409 K (T_g+67 K, n cycles of 12 τ spaced pulses in the dipolar filter); (a) plotted on a linear scale as a function of the square root of the mixing time; (b) plotted on a linear scale as a function of the square of the mixing time; (c) plotted on a logarithmic scale as a function of the mixing time after subtraction of plateau value and normalization.

Figure 7:

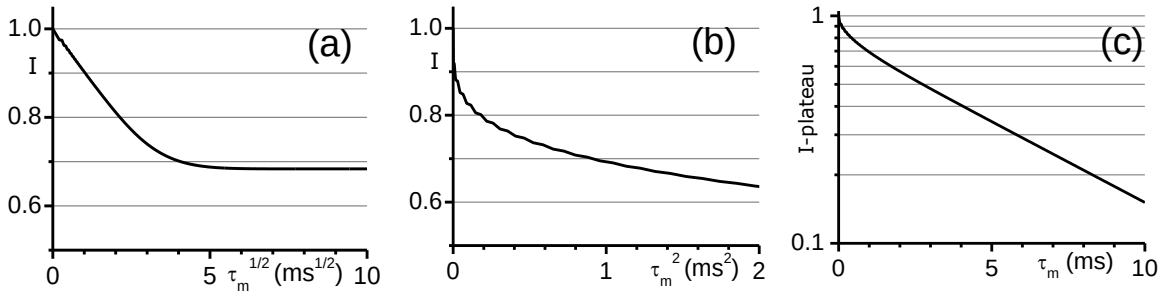

Figure 7: Evolution of the ^{1}H magnetization of mobile species with the mixing time in an ideal case, numerically calculated from theoretical equations [7] (for rigid domains, a dimensionality of 2, a diameter of the source of 5.68 nm, a diffusion coefficient of 0.47 $nm^2 \cdot ms^{-1}$ for both phases, a maximal transition probability of 0.5, a density of 1 for both phases, and a final value of 0.69); (a) plotted on a linear scale as a function of the square root of the mixing time; (b) plotted on a linear scale as a function of the square of the mixing time; (c) plotted on a logarithmic scale as a function of the mixing time after subtraction of plateau value and normalization.

Figure 8:

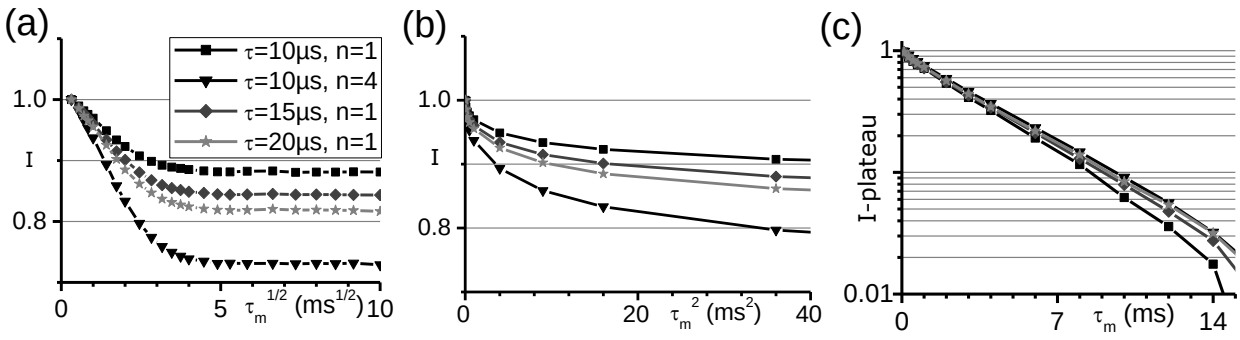

Figure 8: Evolution of the ^{1}H magnetization of mobile species with the mixing time for the sample PEMA at 457 K (T_g+115 K, n cycles of 12 τ spaced pulses in the dipolar filter); (a) plotted on a linear scale as a function of the square root of the mixing time; (b) plotted on a linear scale as a function of the square of the mixing time; (c) plotted on a logarithmic scale as a function of the mixing time after subtraction of plateau value and normalization.

Figure 9:

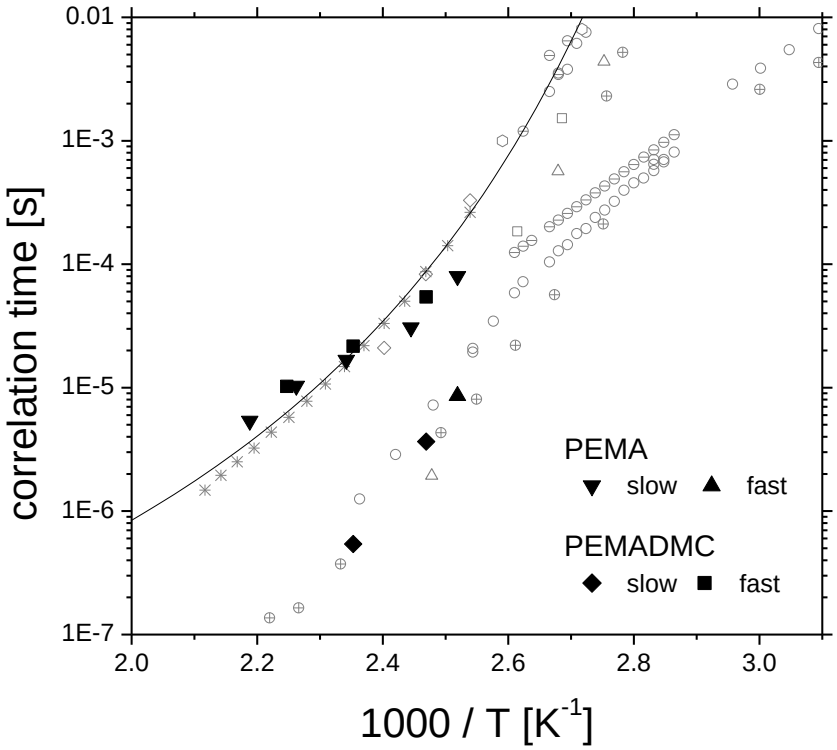

Figure 9: Evolution with the inverse temperature of the correlation time τ_C^{AB} extracted from NOE experiment with dipolar filter for samples PEMA and PEMADMC (the values are assigned to a slow and a fast process in case of bi-exponential magnetization decay). For comparison, data from literature [15] is given in gray symbols.

Figure 10:

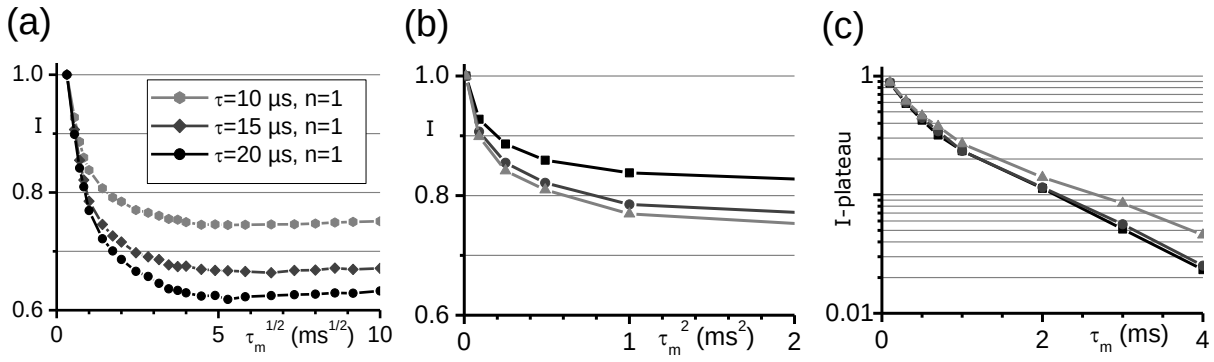

Figure 10: Evolution of the ^{1}H magnetization of mobile species with the mixing time for the sample PEMA at 397 K (T_g+55 K, n cycles of 12 τ spaced pulses in the dipolar filter); (a) plotted on a linear scale as a function of the square root of the mixing time; (b) plotted on a linear scale as a function of the square of the mixing time; (c) plotted on a logarithmic scale as a function of the mixing time after subtraction of plateau value and normalization.